Palaeogeography, Palaeoclimatology, Palaeoecology 426 (2015) 10–21

Contents lists available at ScienceDirect

Palaeogeography, Palaeoclimatology, Palaeoecology

journal homepage: www.elsevier.com/locate/palaeo

Contrasting sea surface temperature of summer and winter monsoon variability in the northern Arabian Sea over the last 25 ka

Anna Böll [a,*], Hartmut Schulz [b], Philipp Munz [b], Tim Rixen [a,c], Birgit Gaye [a], Kay-Christian Emeis [a,d]

[a] Institute of Geology, University of Hamburg, Bundesstr. 55, 20146 Hamburg, Germany
[b] Department of Geosciences, University of Tübingen, Hölderlinstr. 12, 72074 Tübingen, Germany
[c] Leibniz Center for Tropical Marine Ecology, Fahrenheitstr. 6, 28359 Bremen, Germany
[d] Institute of Coastal Research, Helmholtz Center Geesthacht, Max-Planck-Str. 1, 21502 Geesthacht, Germany

ARTICLE INFO

Article history:
Received 2 October 2014
Received in revised form 20 February 2015
Accepted 24 February 2015
Available online 5 March 2015

Keywords:
Sea surface temperature
Arabian Sea
Summer monsoon
Winter monsoon
Holocene
Global climate variability

ABSTRACT

The seasonal monsoon cycle with winds from the southwest (SW) in summer and from the northeast (NE) in winter strongly impacts on modern regional sea surface temperature (SST) patterns in the Arabian Sea (northern Indian Ocean). To reconstruct the temporal and spatial variation in the dynamically coupled winter and summer monsoon strength over the last 25 ka, we analyzed alkenone-derived SST variations in one sediment core from the northwestern Arabian Sea, that is influenced by the summer monsoon (SST affected by upwelling processes), and in one core from the northeastern Arabian Sea, where SST is mainly governed by the winter monsoon (no upwelling). Comparison of the SST records reveals an antagonistic relationship of summer and winter monsoon strength throughout the late deglaciation and the Holocene. Upwelling along the Arabian Peninsula associated with peak SW monsoonal wind strength was strongest during the early Holocene climate optimum between 11 and 8 ka, and coincided with the northernmost position of the Intertropical Convergence Zone (ITCZ) marked by maximum precipitation over northern Oman. The SW monsoon weakened over the middle to late Holocene, while the NE monsoon gained strength. This different evolution was caused by the southward displacement of the ITCZ throughout the Holocene. Superimposed over the long-term trend are variations in northeast monsoon wind strength at time scales of centuries that were synchronous with late Holocene climate variations recorded on the Asian continent and in the high-latitude Northern Hemisphere. Their likely driving forces are insolation changes associated with sunspot cycles. Enhanced by feedback mechanisms (e.g. land-sea thermal contrast) they enforced centennial scale fluctuations in wind strength and temperature in the northern Arabian Sea monsoon system.

1. Introduction

The oceanic environment and surface ocean properties of the Arabian Sea are directly coupled to the seasonal monsoon cycle. Alternating wind directions with low-level winds from the southwest (SW) in summer and from the northeast (NE) in winter cause regional differences in Arabian Sea sea surface temperature (SST) patterns. South-westerly winds are generated by the atmospheric pressure difference between the cold southern Indian Ocean and the heat low over central Asia in spring and summer. They drive upwelling of cold, nutrient-rich waters along the coasts of Somalia, Oman and southwest India and wind-stress curl-driven upwelling offshore (Hastenrath and Lamb, 1979; Rixen et al., 2000). These upwelling regions exhibit sea surface cooling during Northern Hemisphere (NH) summer (Levitus and Boyer, 1994) and high rates of primary production by upwelled nutrients (Haake et al., 1993; Rixen et al., 1996). In the northeastern Arabian Sea off Pakistan, on the other hand, no upwelling occurs and SST remains warm during NH summer. The seasonal SST pattern in the northern Arabian Sea is furthermore governed by the NE monsoon in NH winter. During this part of the year moderately strong, cold and dry north-easterly winds (caused by the reversal of atmospheric pressure gradients between central Asia and the southern Indian Ocean in fall (Clemens et al., 1991)) prevail in this region. The resultant increase in evaporation rates together with a reduction in solar insolation lowers SST and increases the density of surface waters (Madhupratap et al., 1996; Prasanna Kumar and Prasad, 1996). Thus, while SSTs on the Pakistan Margin show a clear seasonal signal with high SST in summer (~28.5 °C) and low SST (~23.5 °C) in winter (Fig. 1C; Levitus and Boyer, 1994), this seasonal pattern is less pronounced on the Oman Margin due to upwelling induced cooling during the summer season (Fig. 1B).

The seasonally variable SST pattern of the Arabian Sea thus reflects monsoon dynamics and relative monsoon strength so that SST changes determined in sediment records track past variations in monsoon

* Corresponding author.
E-mail address: anna.boell@zmaw.de (A. Böll).

http://dx.doi.org/10.1016/j.palaeo.2015.02.036
0031-0182/

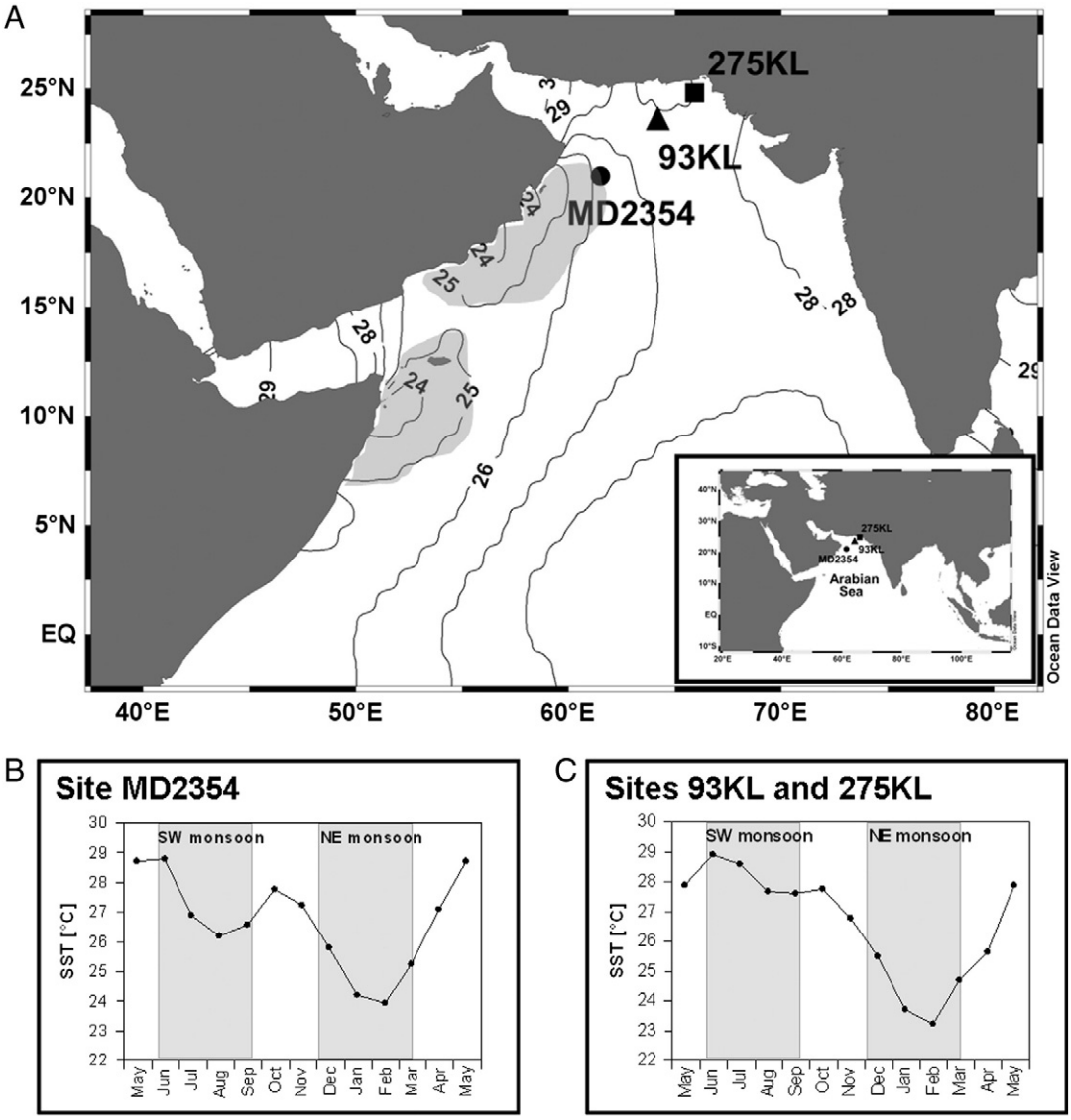

Fig. 1. A) Study area with core location MD00-2354 from the northwestern (NW) Arabian Sea and 93KL and 275KL from the northeastern (NE) Arabian Sea. Illustrated is the sea surface temperature pattern during the summer monsoon season (Jul–Sep). Shaded areas indicate regions of upwelling. This map was produced by using Ocean Data View (Schlitzer, 2013). B) Annual SST variability for site MD2354 and C) sites 93KL and 275KL extracted from the Wold Ocean Atlas (Levitus and Boyer, 1994).

strength over glacial/interglacial cycles (Emeis et al., 1995; Rostek et al., 1997; Schulte and Müller, 2001) and during the Holocene (e.g., Naidu and Malmgren, 2005; Dahl and Oppo, 2006; Huguet et al., 2006; Saher et al., 2007a; Anand et al., 2008; Saraswat et al., 2013). From these reconstructions, a general pattern emerged of increased NE monsoon strength during cold glacial stages and stadials, and vigorous SW monsoon strength during warm interglacials and interstadial periods (e.g., Rostek et al., 1997; Reichart et al., 1998; Schulz et al., 1998; Schulte and Müller, 2001; Wang et al., 2001). This change in wind patterns had consequences beyond SST: Interglacials and interstadials also marked productivity maxima and an expanded oxygen minimum zone (OMZ) with intense denitrification in the Arabian Sea subthermocline, as reflected in maxima of organic carbon burial and $\delta^{15}N$ in sediments (Suthhof et al., 2001; Altabet et al., 2002). Monsoon activity in the Arabian Sea region varied on Milankovitch and millennial time scales not only during the Pleistocene, but also (with smaller amplitude) during the Holocene (e.g., Sirocko et al., 1993; Overpeck et al., 1996; Lückge et al., 2001; Anderson et al., 2002, 2010; Gupta et al., 2003, 2011; Fleitmann et al., 2004). Strongest SW monsoon activity was recorded in the early Holocene insolation maximum when air temperatures (Marcott et al., 2013) and summer precipitation in Asia were high (Fleitmann et al., 2003; Herzschuh, 2006). Most of these studies aimed to reconstruct summer monsoon strength, that determines the state of the upwelling system in the western Arabian Sea (Naidu and Malmgren, 1996; Anderson et al., 2002, 2010; Gupta et al., 2003). Much less attention has been given to the response of the NE monsoon to changing mid-latitude glacial/interglacial boundary conditions, and the dynamic evolution of the coupled winter and summer monsoon throughout the Holocene (Reichart et al., 2002; Yancheva et al., 2007; Liu et al., 2009).

Since SST provide a signal for both monsoon seasons (i.e., determined by the intensity of summer upwelling versus deep winter mixing), several authors reconstructed time series of seasonal SST variations to distinguish between summer and winter monsoon strengths (Naidu and Malmgren, 2005; Saher et al., 2007b; Anand et al., 2008). An alternative approach was used by Dahl and Oppo (2006), who investigated the spatial SST history of the Arabian Sea basin for different time slices. These authors showed that comparing SST variations in areas today affected by upwelling with areas not affected by upwelling is a viable approach to distinguish sea surface cooling caused by SW monsoonal upwelling from cooling caused by the northeasterly winds of the winter monsoon.

Here we add to this knowledge by presenting two new high-resolution alkenone-based SST records, one from the northern Oman Margin and one from the Pakistan Margin, spanning the last deglaciation and Holocene period. Alkenones are a robust and well studied indicator for past SST changes, but there are yet only a few alkenone-based SST records that document the Holocene SST history of the Arabian Sea (Sonzogni et al., 1998; Schulte and Müller, 2001; Huguet et al., 2006), and none of them with sufficient resolution or location to track Holocene changes in upwelling intensity. By comparing our high-resolution alkenone-based SST record from the northern Oman Margin (SST affected by upwelling processes, Fig. 1B) with that from the Pakistan Margin (no upwelling, Fig. 1C) we aim to disentangle SST signals of the SW and NE monsoon to examine the relationship between both monsoon seasons over the last 25 ka. We furthermore seek for SST signals that (1) would document a response of the NE monsoon to changing glacial/interglacial boundary conditions and (2) would imply an influence of Asian and high-latitude Northern Hemisphere climate on northeast monsoonal wind strength during the Holocene epoch. To these ends, we compared our SST record of the last 25 ka (this study) together with our previously published high-resolution SST record of the late Holocene (Böll et al., 2014), both from the northeastern Arabian Sea, with records of air temperature variability from Asia and the NH, as well as with records of NH solar insolation.

2. Material and methods

2.1. Sediment cores

Piston core 93KL (23°35′N, 64°13′E; 1802 meter water depth) was collected in 1993 during SONNE cruise 90 from the northern Murray Ridge near the coast of Pakistan (Schulz et al., 1998, 2002; von Rad et al., 2002). Calypso Core MD00-2354 (21°02.55′N, 61°28.51′E; 2740 meter water depth) was obtained from the northernmost section of the Owen Ridge, ~210 km offshore the Oman Margin by the research vessel MARION DUFRESNE in 2000. Both cores were sampled in 2.5 cm intervals (sample resolution of 100 to 300 years in core MD2354 and ~100 years in core 93KL) and alkenone unsaturation ratios were measured at the Institute for Baltic Sea Research Warnemünde (see below). Core SO130-275KL representing the late Holocene was analyzed at the Institute of Geology in Hamburg and results were published by Böll et al. (2014).

2.2. Stratigraphy

Pronounced sediment facies changes between laminated, organic carbon rich and bioturbated, hemipelagic sediments are observed in the northern Arabian Sea at shallow to intermediate water depths within the oxygen-minimum zone off Pakistan. Their relative dominance varied in phase with Northern Hemisphere climate depicted by the Greenland ice cores (e.g., Grootes and Stuiver, 1997). The change in depositional conditions is also seen in cores from deeper water and is represented by various sediment properties, such as sediment color, sediment geochemistry, or physical properties.

2.2.1. Core SO90-93KL

A detailed chronology of core SO90-93KL, based on a correlation of sediment facies to the GISP2 ice core record has been published by Schulz et al. (1998, 2002) for the past 110,000 years.

2.2.2. Core MD00-2354

Sirocko et al. (1993) recognized and dated (12 AMS ^{14}C dates) a series of events in the high-resolution planktonic δ^{18}O record of the northern Arabian Sea core 74KL over the last 25 ka (see Table 1 in Sirocko et al., 1993). For the present study, that stratigraphic framework (using these parameters in addition to δ^{18}O stratigraphy) has been adopted. 5 to 25 specimens of *Globigerinodes ruber* white were picked from the 315–400 μm size fraction. Tests were cracked and cleaned in methanol and ultrasonic bath and were analyzed at the Kiel University Leibniz Institute for isotope research. Our δ^{18}O record of core MD2354 was correlated to the GISP 2 ice core record and to the δ^{18}O stratigraphy of Arabian Sea core 74KL using these events as stratigraphic match points (see Table 1 and Fig. S1 in the supporting information). The stable planktic isotope record of core MD2354 matches well with other Arabian Sea records and displays the established scheme of the two-step deglaciation with rapid shifts in δ^{18}O centered at ~15.0 and 11.0 ka BP, framing a ~3 ka-long plateau of δ^{18}O values of −0.7‰ (MD2354) and −1.0‰ (93KL and 74KL) (Fig. S1b). We estimate that the precision of our approach is less than 1 ka, and thus comparable to individual AMS ^{14}C dating (where available) of stratigraphic match points.

Table 1
Age model (0–25 ka) for Arabian Sea core MD00-2354.

GISP 2	MD00-2354	Comment
Age (ka BP)	Depth (cm)	
1.00[a]	0.0	Core top
9.7[5]	80.0	Start early Holocene
11.45[4]	115.0	Start termination IB
12.6	130.0	Younger Dryas Maximum
12.9	142.5	Younger Dryas Start
14.5	165.0	IS1 = B/A maximum
16.1[3]	197.5	H1 maximum
17.2[2]	227.5	H1 base
23.3	297.5	IS 2
24.0	375.0	H2 maximum
24.7	390.0	H2 midpoint

5, 4, 3, 2 correlative isotope events to Sirocko et al. (Table I, 1993).
B/A = Bølling/Allerød epoch, IS = interstadial, H = Heinrich chronozones.
[a] Suggested age of intact core top, indicated by brownish-colored top layer.

2.3. Alkenone analysis

Sample preparation and analytical methods for alkenone analysis of cores SO90-93KL and MD2354 are detailed in Emeis et al. (2000). Subsamples of 1–3 g sediment were extracted twice for 10 min with methylene chloride (DCM) by ultrasonic agitation. The combined extracts were fractionated using high pressure liquid chromatography (HPLC) on a silica gel column (MERCK LiChrosphere Si 100-5) with four elution steps of increasing polarity. The alkenones were isolated in the second fraction (n-hexane/DCM [90:10; v/v]). Alkenones were analyzed by gas chromatography on a HR 8000 Finsons gas chromatograph equipped with a cold on-column injection system and a flame ionization detector. Alkenones were separated on a 30 m glass capillary column (DB5HT) using hydrogen as carrier gas.

Sample preparation and analytical methods for core 275KL are those in Böll et al. (2014). Replicate extraction and measurement of a working sediment standard resulted in a mean standard deviation of estimated SST of 0.5 °C. The alkenone index for all cores was translated to SST using the Indian Ocean core top equation of Sonzogni et al. (1997): $SST = (U^{K'}_{37} - 0.043) / 0.033$ with $U^{K'}_{37} = C_{37:2} / (C_{37:2} + C_{37:3})$.

3. Results

Alkenone-derived SST estimates agree well with modern annual mean SST in the Indian Ocean (Sonzogni et al., 1997), and in our records the SST at site 93KL (NE Arabian Sea off Pakistan) ranged between 23.2 °C (~18 ka) and 28.0 °C (~8 ka) over the last 25 ka (Fig. 2B). In the interval representing the last glacial in core 93KL in the NE Arabian Sea, SST was high (25 to 26 °C) during the Bølling–Allerød and Dansgaard–Oeschger event 2 and low (23 to 24 °C) during Heinrich events 1 and 2 (H1, H2; see also Fig. 3D). The Last Glacial Maximum (LGM; 23–18 ka) to Holocene transition started at about 17 ka and is marked by a temperature increase of 4 °C, which is slightly higher than the temperature increase found in other Arabian Sea alkenone-

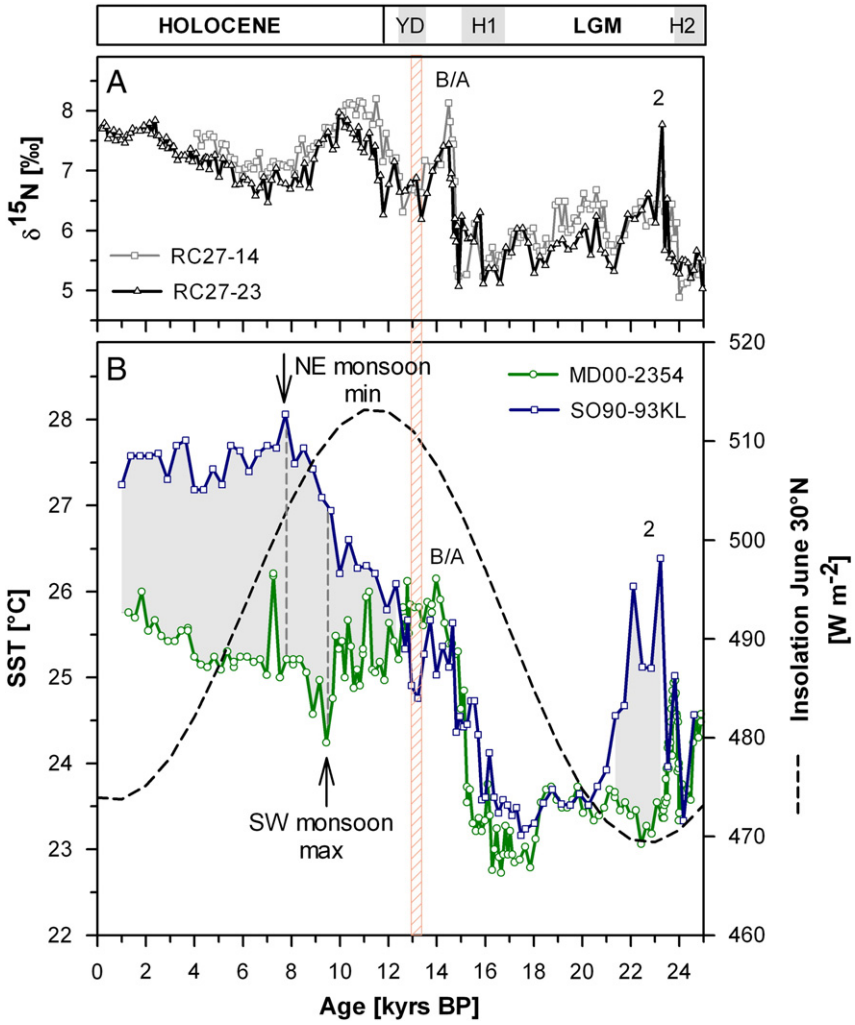

Fig. 2. A) $\delta^{15}N$ record of cores RC27-23 and RC27-14 from the Oman Margin (Altabet et al., 2002), B) alkenone-derived SST reconstruction for the northwestern Arabian Sea (core MD00-2354) and for the northeastern Arabian Sea (core 93KL). Both SST records are equally affected by winter cooling but only SST at site MD2354 is influenced by upwelling-induced cooling. Gray shading indicates the occurrence of upwelling at site MD2354. Dashed gray lines indicate the timing of maximum SW and minimum NE monsoon strength, respectively. Further illustrated are Heinrich events (H1 and H2), Dansgaard–Oeschger event 2, the Bølling–Allerød (B/A) and the Younger Dryas (YD; stippled red area).

SST reconstructions (Emeis et al., 1995; Rostek et al., 1997; Sonzogni et al., 1998; Schulte and Müller, 2001; Pourmand et al., 2007). After a maximum at 8 ka during the early Holocene SW monsoon maximum, SST was relatively stable and showed a slight decrease until today. The general Holocene SST trend seen in core 93KL is similar to the SST reconstruction of the nearby core 136KL (Fig. 3C; Schulte and Müller, 2001). Since the SST history of the last 2.5 ka is not very well resolved in core 93KL, alkenone-SST data from the recently published, nearby high-resolution core 275KL (Böll et al., 2014) were used to better resolve the late Holocene SST evolution. That record reveals a late Holocene SST cooling trend in the NE Arabian Sea, in line with the long-term temperature trend seen in core 93KL.

The range of SST at site MD2354 in the NW Arabian Sea (between 22.7 °C (~16.5 ka) and 26.1 °C (14 and 7 ka)) is smaller than SST variations observed in core 93KL (Fig. 2B). SST at both study sites was similarly low during the late LGM (20 to 18 ka) and H1, but showed a different evolution over Interstadial 2, when SST increased at site 93KL but remained low at site MD2354. On the other hand, SST at site MD2354 evolved simultaneously with SST at site 93KL during the transition to Holocene conditions and increased by up to 3 °C from 17 to 15 ka. But whereas SST continued to rise until 8 ka at site 93KL, SST at site MD2354 reached maximum temperatures at ~14 ka. This maximum in SST at site MD2354 was followed by a SST decrease to 24.5 °C at around 9.5 ka. This SST decrease signal intensified upwelling caused by enhanced SW monsoon strength during the early Holocene (e.g., Sirocko et al., 1993; Naidu and Malmgren, 1996; Gupta et al., 2003). Following peak intensity during the Holocene climate optimum, upwelling and, by inference, wind strength weakened and SST gradually increased at site MD2354 off northern Oman.

4. Discussion

4.1. Dynamic evolution of SW and NE monsoon intensity during the last 25 ka

Both the NE (site 93KL) and NW Arabian Sea (site MD2354) experienced low SSTs during the last glaciation compared to Holocene values (Fig. 2B). This glacial situation was interrupted by a temperature increase at site 93KL during IS 2. Other late Quaternary reconstructions of temperatures in the Arabian Sea mixed layer (Rostek et al., 1997; Schulte and Müller, 2001; Naidu and Malmgren, 2005; Dahl and Oppo, 2006; Huguet et al., 2006; Saher et al., 2007a,b; Anand et al., 2008; Saraswat et al., 2013) also evidence basin-wide low SSTs during the LGM (23 to 18 ka; Fig. 3). Similar annual mean SST of sites 93KL and MD2354 indicates that this cooling was controlled by glacial boundary conditions and intensified NE monsoon strength, and not by intense upwelling (Emeis et al., 1995; Schulz et al., 1998; Schulte and Müller, 2001). SST at both of our study sites today is equally affected by the

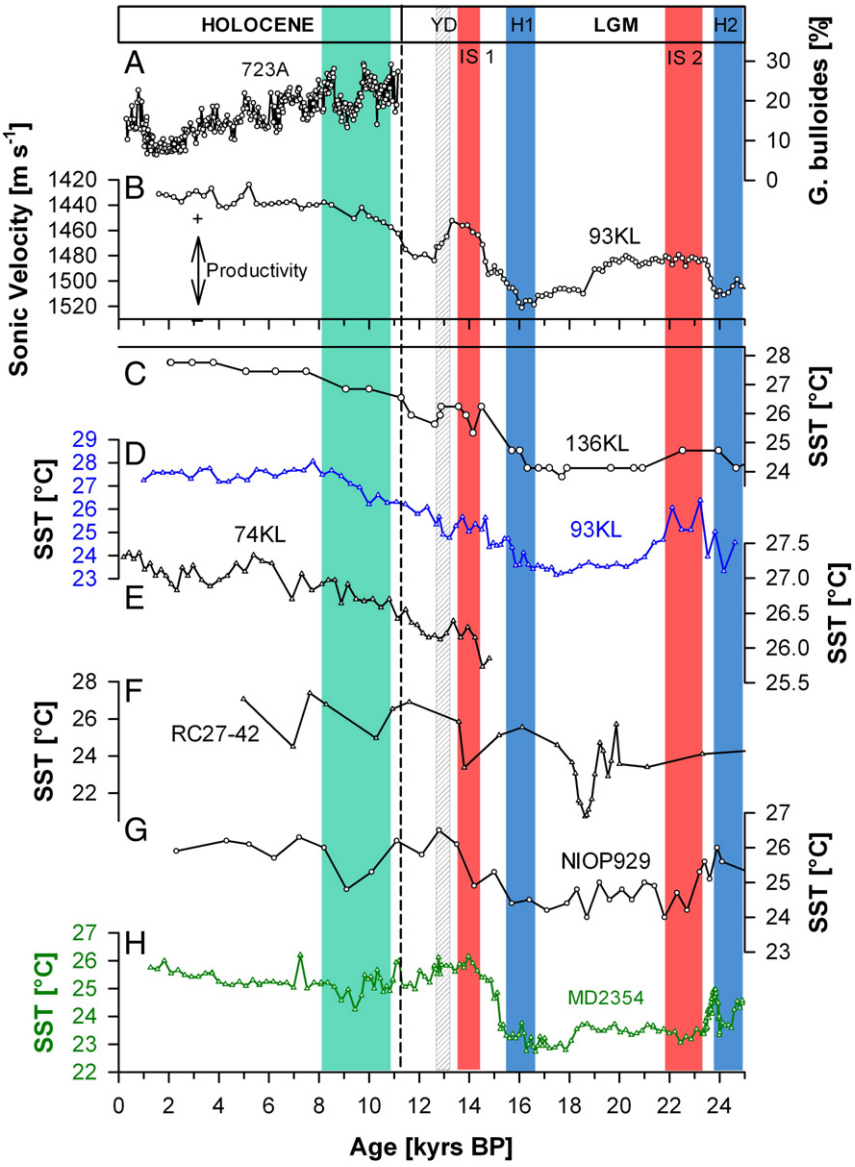

Fig. 3. Comparison of Arabian Sea SST and monsoon records over the last 25 ka. A) *G. bulloides* percentage of core 723A as an indicator for upwelling and monsoon intensity (Gupta et al., 2003) and B) sonic velocity record of core 93KL as a primary productivity indicator (Schulz et al., 1998). Alkenone-derived SST records of C) core 136KL (Schulte and Müller, 2001), D) core 93KL (this study), E) core 74KL (Huguet et al., 2006), F) core RC27-42 (Pourmand et al., 2007), G) core NIOP929 (Rostek et al., 1997) and H) core MD2354 (this study). Shaded areas illustrate major climate events: Heinrich events 1 and 2 (blue), interstadial 1 and 2 (red), the Younger Dryas (YD, dashed gray) and the early Holocene summer monsoon maximum (green).

NE monsoon in winter, but SW monsoonal upwelling in summer lower annual mean (AM) SST at site MD2354 compared to site 93KL (Fig. 1B, C). The past onset of upwelling processes in the northern Arabian Sea thus should be reflected in an AM SST difference between our two study sites (i.e. lower AM SST at site MD2354 compared to site 93KL; see also gray shaded areas in Fig. 2B).

One further argument against intensified upwelling and high primary production during the LGM is the variation in $\delta^{15}N$, an indicator for the extent of denitrification in the OMZ. Low $\delta^{15}N$ values were recorded from 21 to 15 ka at the upwelling sites RC27-23 and 14 and suggest a less intense OMZ and significant reduction or even absence of mid-water denitrification than in the modern situation (Altabet et al., 2002), most likely associated with reduced particle export from the mixed layer (Fig. 2A). Thus, summer monsoon and upwelling induced primary productivity was low over the last glaciation in the northern Arabian Sea. Given the northern position of core MD2354, glacial SST at this site may have further been biased by lateral advection of alkenones produced on the Pakistan Margin via mixed layer deepening under strong NE monsoon conditions. This is, however, very unlikely because down core studies offshore Pakistan showed no indication of enhanced primary (and alkenone) production over glacial and stadial stages (see Fig. 3B; Schulte and Müller, 2001; Schulz et al., 1998) and sediment focusing or winnowing did not occur at our study sites (Pourmand et al., 2004, 2007).

The strong SST contrast between sites 93KL and MD2354 from 23 to 21.5 ka together with high $\delta^{15}N$ at sites RC27-23/14 reveals that this glacial situation was interrupted by upwelling processes in the northern Arabian Sea during IS 2 (Fig. 2A, B). While diminished north-easterly winds caused a SST increase at site 93KL off Pakistan during this period, the SST increase was suppressed at site MD2354 due to the intensification of SW monsoon winds and the accompanied onset of upwelling offshore northern Oman. Strengthening SW monsoon conditions during IS 2 are also indicated by the contemporaneous increase of primary productivity in the northern Arabian Sea between 23 and 20 ka (Schulz et al., 1998; Schulte and Müller, 2001; Pourmand et al., 2004). This apparent inverse behavior of summer and winter monsoon seen in our

record over the last glaciation (strong summer monsoon/weak winter monsoon intensity during warm climate periods such as IS 2 and weak summer monsoon/strong winter monsoon during cold periods such as Heinrich events 1, 2 and the LGM) is probably linked to the strength and position of the mid-latitude westerlies. Under cold climate conditions the mid-latitude westerlies intensify and move southward, thus enhancing the strength of the winter monsoon. They retreat northward and loose strength during warm climate intervals when the summer monsoon gets stronger (Fang et al., 1999).

The northern Arabian Sea began to warm at about 17 ka, most likely as a result of weakening NE monsoon forcing together with strengthening SW monsoon winds. This SST rise lagged the increase of NH solar insolation by about 5000 years and can be attributed to glacial boundary conditions and NE monsoon forcing (Fig. 2B). Both of our study sites display similar warming trends between 17 and 14 ka, because SW monsoonal winds were too weak to induce upwelling at site MD2354. Other SST reconstructions from the upwelling region of the northern Arabian Sea (Rostek et al., 1997; Huguet et al., 2006; Saher et al., 2007a,b) show the same onset of warming and a comparable SST trend over the last deglaciation and support this interpretation (Fig. 3). The overall increase in SST was interrupted by a short-term period of SW monsoon weakening (and/or NE monsoon strengthening) induced by NH cooling during the Younger Dryas, which is expressed in decreased precipitation in Oman (Fuchs and Buerkert, 2008) and northeast Asia (Wang et al., 2001; Dykoski et al., 2005), and also by reduced upwelling (relatively low $\delta^{15}N$, see Fig. 2A (Altabet et al., 2002)) and low organic carbon flux rates in the Arabian Sea (e.g., Schulte and Müller, 2001; Ivanochko et al., 2005). Whereas SST in the NE Arabian Sea (site 93KL) gradually increased until 8 ka due to weakening NE monsoon strength, SST off Oman (site MD2354) decreased after its maximum during the Bølling–Allerød at ~14 ka. Significant lower SST at site MD2354 than at site 93KL since 13 ka marks the onset of oceanic conditions in the northern Arabian Sea that are characterized by SW monsoon induced upwelling offshore Somalia and Oman (gray shaded area in Fig. 2B). Thus, the SST decrease from 14 to 9.5 ka at site MD2354 tracks intensified upwelling offshore Oman caused by invigorated SW monsoon winds.

Our alkenone-derived SST record is the first one in high-resolution to confirm an early Holocene upwelling increase with a SST minimum. A slight decrease in SST on the Oman Margin is also documented by the low-resolution core NIOP929 (Rostek et al., 1997) over the early Holocene, but SSTs at site 74KL (Huguet et al., 2006) show no indication of intensified upwelling (Fig. 3E, F). Nevertheless, the SST estimate from core MD2354 of 24.5 °C at ~9.5 ka suggests that upwelling was much more vigorous than today, because modern annual average SST is around 26 °C in the Oman upwelling area (Levitus and Boyer, 1994). Other evidence, such as peak abundances of *Globigerina bulloides* (Fig. 3A; Gupta et al., 2003; Naidu and Malmgren, 1996) and maximum $\delta^{15}N$ (Suthhof et al., 2001; Altabet et al., 2002) also suggests that upwelling and thus summer monsoon strength were intense during the early Holocene. Terrestrial records, moreover, indicate an early Holocene SW monsoon maximum throughout the Asian monsoon domain: Wet climate conditions with high rates of summer monsoonal rainfall were recorded in southern China (Dykoski et al., 2005), India (Kessarkar et al., 2013), Oman (Fleitmann et al., 2003, 2007; Fuchs and Buerkert, 2008) and Yemen (Lézine et al., 2007). Fleitmann et al. (2007) and Van Rampelbergh et al. (2013) pointed out that maximum rainfall in southern and northern Oman cave records is related to a shift of the northernmost position of the Intertropical Convergence Zone (ITCZ) to northern Oman. We believe that this has not only intensified, but also led to a longer duration of seasonal upwelling.

The early Holocene upwelling intensification indicated by SST cooling at site MD2354 is in line with the $\delta^{15}N$ record from the Oman Margin during the period from 12 to 10 ka (Fig. 2A). High $\delta^{15}N$ values during this time indicate intensified denitrification in an expanding OMZ caused by enhanced particle export from the mixed layer due to increased upwelling strength. But this period was followed by an interval of decreasing $\delta^{15}N$ from 10 to 9 ka that is embedded in the decreasing temperature trend (Fig. 2A, B). The deviation from the long-term (glacial–interglacial) antagonistic pattern of SST and $\delta^{15}N$ is in our interpretation due to adjustments in intermediate water mass origin and circulation in the northern Arabian Sea. Pichevin et al. (2007) pointed out that the extension and position of the OMZ are the expression of an interplay between productivity and ventilation, and Rixen et al. (2014) showed that enhanced upwelling is accompanied with enhanced inflow of well-ventilated Indian Central Water into the OMZ from the south. Furthermore, sea level rise in the early Holocene triggered the outflow of Persian Gulf intermediate water into the thermocline of the Arabian Sea, which today adds to OMZ ventilation (Lambeck, 1996).

Temperatures in the sea surface of the NE Arabian Sea (site 93KL) evolved differently. Over the time of maximum upwelling and SW monsoon strength in the SW Arabian Sea from 12 to 9 ka, SSTs here continue to rise and indicate waning NE monsoon strength. This decoupling of conditions in the mixed layers over the Oman and Pakistan margins on sub-Milankovitch time scales (as indicated in SST variations; Fig. 2B) has been previously observed in productivity records (Reichart et al., 2002).

SST at site MD2354 increased again over the middle to late Holocene (since ~8 ka) but slightly decreased at site 93KL pointing to a decline in SW monsoon strength (weakened upwelling) at invigorated NE monsoon conditions as a response to decreasing NH summer solar insolation (e.g., Neff et al., 2001; Fleitmann et al., 2003; Gupta et al., 2005). This slight increase of NE monsoon conditions during the late Holocene parallels strengthened winter mixing in the northeastern Arabian Sea that induced high primary productivity at site 93KL (Fig. 3B). On the other hand, the gradual Holocene decrease of SW monsoon intensity that is evidenced by our SST record (site MD2354) supports the well-established picture of Arabian Sea summer monsoon evolution over the Holocene (e.g., Overpeck et al., 1996; Gupta et al., 2003; Fleitmann et al., 2007). Over this period intense (weak) winter monsoon activity in the northern Arabian Sea (site 93KL) coincides with strong (weak) East Asian winter monsoons (Yancheva et al., 2007). Minimum NE monsoon intensity (~8 ka), however, occurred 1500 years later than peak SW monsoon strength (~9.5 ka) and the general opposing trend of summer and winter monsoon activity was less clear between 9.5 and 8 ka (Fig. 2B). Sedimentary alkenone SST records represent an annually integrated SST signal over several years of sediment deposition, so that small differences in the exact timing of minimum and maximum temperatures between both regions are to be expected. This antagonistic pattern of summer and winter monsoon variability is best explained by long-term movements of the annual mean position of the ITCZ (Yancheva et al., 2007), as proposed previously by Böll et al. (2014) for the late Holocene. Northern Hemisphere cooling in response to decreasing solar irradiance moves the mean position of the ITCZ southward (Broccoli et al., 2006), thus reducing the northward extent of the Asian SW monsoon and reducing summer monsoon precipitation over the Asian continent (Yancheva et al., 2007). The northern Arabian Sea is located within the northern limit of the long-term annual mean position of the ITCZ, so that long-term southward displacement of the ITCZ throughout the Holocene (Haug et al., 2001) shortens the summer monsoon season and strengthens or prolongs the influence of NE monsoon winds over the northern Arabian Sea, causing low annual mean SST off Pakistan (site 93KL). Insolation-triggered ITCZ movements thus do not only affect the rainfall patterns over land, but apparently also influence upper ocean properties in the northern Arabian Sea by modulating monsoon strength.

4.2. Monsoon variability in the NE Arabian Sea and Asian air temperature variations during the last deglaciation and over the last 2500 years

SST offshore Pakistan today is strongly influenced by ocean–atmosphere interaction. Comparison of our northern Arabian Sea SST record

(site 93KL) with records of air temperature variability from Asia (Thompson et al., 1997; Wen et al., 2010; Peterse et al., 2011) shows that this relationship was less pronounced during the last deglaciation (Fig. 4B, C). Whereas air temperatures recorded on the Asian continent closely tracked NH summer solar insolation during the last deglaciation (Fig. 4B), maximum SST at site 93KL (and thus minimum NE monsoon strength) in the NE Arabian Sea lagged air temperature and maximum solar insolation by about 3.5 ka (Fig. 4C). Longer records have shown that the timing of maximum summer monsoon strength lagged peak NH summer solar insolation by ~8 ka at the precession band over the last 350,000 years (e.g., Clemens and Prell, 2003; Wang et al., 2005a; Clemens et al., 2010). However, high-resolution records indicate a phase lag of about 2–3 ka between maximum summer monsoon strength and peak summer solar insolation for the last glacial to Holocene transition (Overpeck et al., 1996; Dykoski et al., 2005; Fleitmann et al., 2007), that is in line with our SST data from the northern Arabian Sea. This lag has been attributed to internal climate forcing by glacial boundary conditions, such as North Atlantic temperature and global ice coverage and to the extent of latent heat export from the southern subtropical Indian Ocean associated with the precession and obliquity band (Clemens and Prell, 2003).

Monsoon intensity off Pakistan (site 93KL) apparently was still influenced by glacial boundary conditions during the last deglaciation that suppressed direct insolation forcing on monsoon intensity and thus SST. Slightly decreasing SST at site 93KL indicative of increased NE monsoon strength off Pakistan from about 8 to 4 ka (Fig. 4C), on the other hand, matches very well with contemporaneous cooling on the Tibetan Plateau as indicated by a depletion of ice core $\delta^{18}O$ in the Guliya ice cap (Fig. 4B; Thompson et al., 1997). This would imply that during the mid to late Holocene, when glacial boundary conditions were negligible, NE monsoon intensity in the NE Arabian Sea may have directly (and without a time lag) responded to atmospheric forcing, such as air temperature and solar insolation. To test this hypothesis for centennial scale climate variability, below we compared our previously published, high-

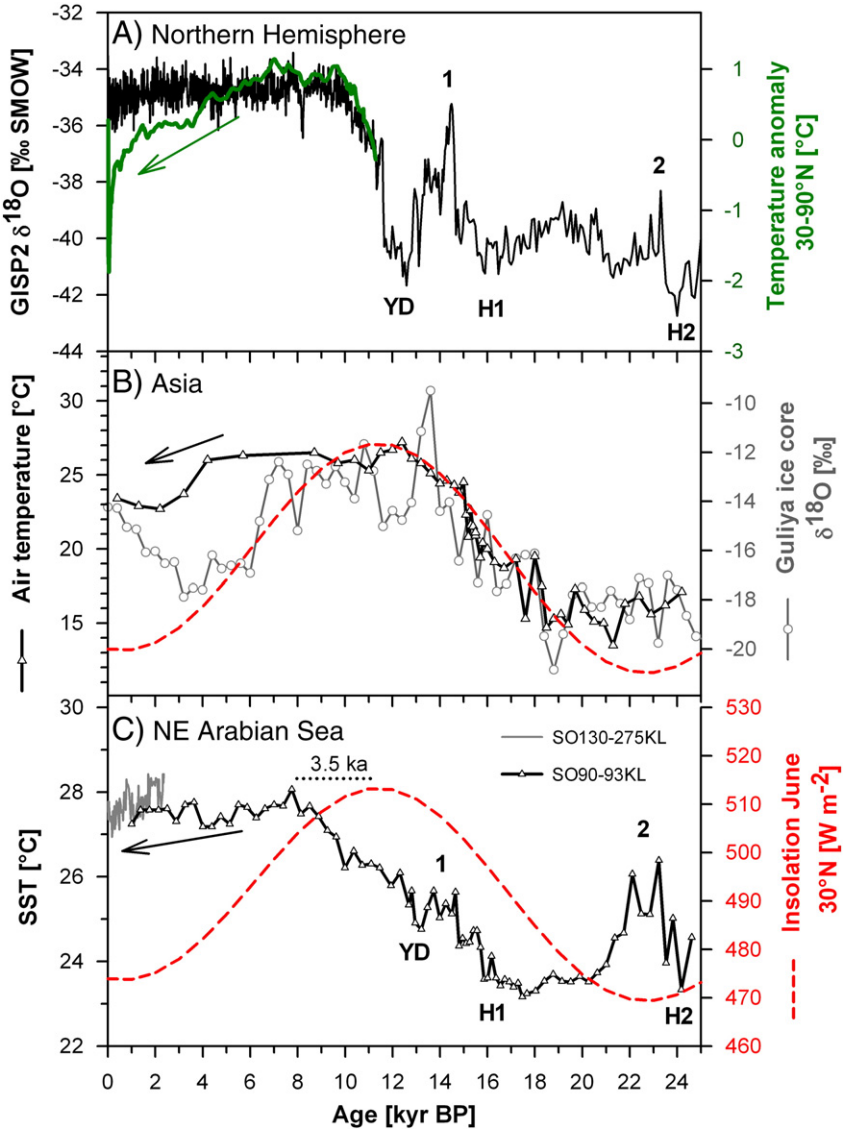

Fig. 4. SST variations in the northeastern Arabian Sea over the last 25 ka compared to air temperature variations in Asia and the Northern Hemisphere. A) temperature reconstructions for the North Atlantic (GISP2 ice core; Grootes and Stuiver, 1997) (black line) and the extratropical Northern Hemisphere (30°N–90°N; Marcott et al., 2013) (green line), B) record of continental air temperature for central China (black curve; Peterse et al., 2011) and the Tibetan Plateau (gray curve; Thompson et al., 1997) compared to Northern Hemisphere (NH) summer solar insolation (Berger and Loutre, 1991) (red curve; same scale as in 3C) and C) alkenone-derived SST reconstructions of core 93KL (last 25 ka) and cores 39KG/275KL (last 2.5 ka; Böll et al., 2014) compared to NH summer solar insolation (red curve; Berger and Loutre, 1991).

resolution SST reconstruction of core 275KL (Böll et al., 2014) with air temperature variations recorded in Asia over the last 2000 years (Fig. 5). Although the amplitude of SST variability is small in core 275KL, this record exhibits significant periods of long-term SST changes (a detailed discussion of the signal-to-noise ratio is given in Böll et al., 2014).

Comparison of alkenone-SST from the northeastern Arabian Sea (core 275KL; Böll et al., 2014) with temperature reconstructions from Asia (PAGES 2k Consortium, 2013) and China (Ge et al., 2013) reveals similar century-long temperature trends over the last 2000 years (Fig. 5). Periods of generally increased (decreased) SSTs in the NE Arabian Sea coincided with warm (cold) temperature excursions in China (see dashed lines in Fig. 5). In general, both regions exhibited relatively warm climate conditions during NH warm periods such as the Roman Warm Period (RWP) and Medieval Warm Period (MWP), as well as recent warming over the last 100 years. On the other hand, a trend to colder climatic conditions is registered in both records during the Little Ice Age (LIA) from 0.55 to 0.1 ka (1400 to 1850 A.D.), whereas climate was more variable in China and this relationship was less significant from 1.55 to 1.15 ka (400 to 800 A.D.).

These coherent temperature changes between the NE Arabian Sea and the Asian continent (Esper et al., 2002; Yang et al., 2002; Bao et al., 2003; Ge et al., 2013; PAGES 2k Consortium, 2013) imply a strong linkage between land and ocean during the last two millennia by the Asian monsoon system. Low SSTs on the Pakistan Margin indicate times of strengthened NE monsoonal winds in winter and/or weaker SW monsoon in summer (see Section 4.1). Modeling studies suggest that low air temperatures over Pakistan, north-west India and beyond were associated with strong north-easterly monsoon winds, the advection of cold, dry air over the Arabian Sea and low SST in the northern Arabian Sea during boreal winter (Marathayil et al., 2013). Thus, cold climate conditions over land during the LIA (Fig. 5A, C) (Esper et al., 2002; Yang et al., 2002; Ge et al., 2013; PAGES 2k Consortium, 2013) increased NE monsoonal wind strength over the NE Arabian Sea and caused low SST off the coast of Pakistan (Fig. 5B). Centennial scale variations in NE monsoon strength over the NE Arabian Sea were thus directly influenced by Asian climate via atmospheric teleconnections over the mid to late Holocene.

4.3. NE monsoon intensity and Northern Hemisphere climate change

Monsoon strength is closely coupled to North Atlantic climate over glacial/interglacial cycles, but Holocene millennial scale changes in NE monsoon intensity (core 93KL, Fig. 4B) are not reflected in GISP2 ice core data (Grootes and Stuiver, 1997) that indicate relative stable climate conditions over the Holocene (Fig. 4A). Nevertheless, a recently published multi-proxy temperature reconstruction from the extratropical NH (Marcott et al., 2013) exhibits gradual NH cooling since the beginning of the Holocene that parallels strengthening of NE monsoon intensity over the NE Arabian Sea (as indicated by lowered SST at site 93KL; Fig. 4A, C). The NE monsoon was weak during the early Holocene when temperatures in the extratropical NH (30°N to 90°N) were high. On the other hand, decreasing temperatures in the NH from 5.5 to 0.1 ka match strengthened winter monsoon intensity over the northern Arabian Sea and East Asia (Yancheva et al., 2007). This linkage was also recognized in variations in summer monsoon strength and related to NH climate during the Holocene (e.g., Gupta et al., 2003; Hong et al., 2003; Wang et al., 2005b).

Similar features of the high-resolution SST record from core 275KL and NH temperature reconstructions suggest that the linkage between

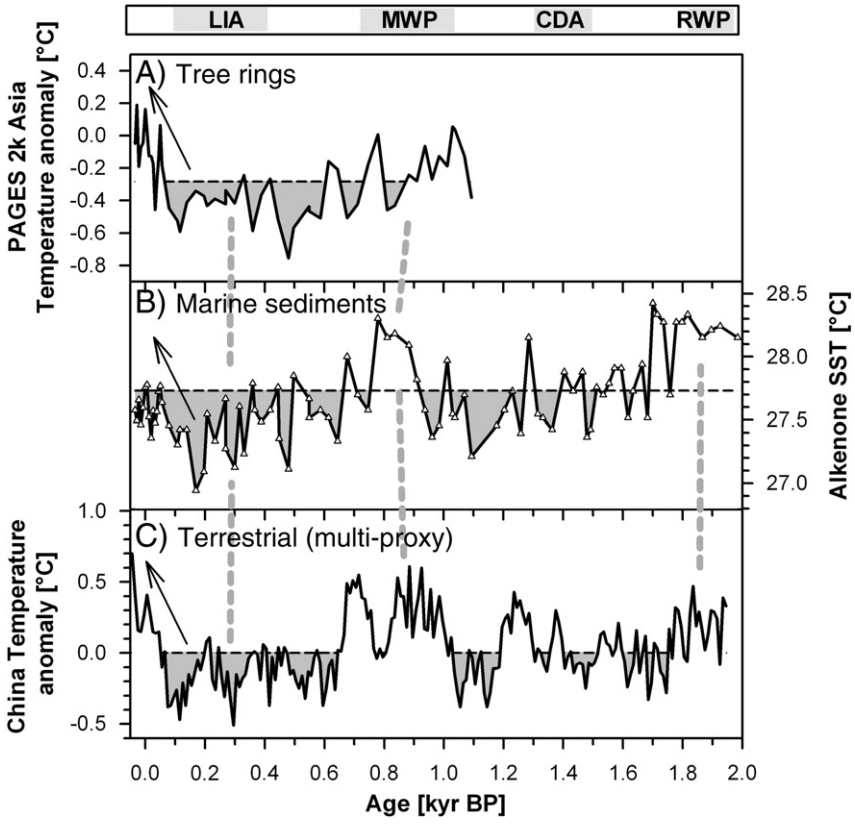

Fig. 5. Temperature variability over the Asian monsoon domain during the last two millennia derived from A) tree-rings (smoothed by calculating the respective mean value over the time interval which is represented by the alkenones) from PAGES 2k Consortium (2013), B) marine sediments from the northeastern Arabian Sea (alkenone-derived SST in core 39KG/275KL; Böll et al., 2014) and C) a combination of different continental proxy types (Ge et al., 2013). Dashed lines indicate the respective mean over the studied time interval. Dashed gray lines suggest correlations between the archives. Further illustrated are characteristic climate periods known from the Northern Hemisphere: Little Ice Age (LIA), Medieval Warm Period (MWP), Cold Dark Ages (CDA) and Roman Warm Period (RWP).

Asian climate variability and high-latitude climate change also exists on centennial time scales during the late Holocene (Fig. 6). Variations in NE monsoon strength in the NE Arabian Sea (core 275KL; Fig. 6D) are similar to air temperature variability over Central Greenland (Fig. 6B; Alley, 2000) and the entire NH (Fig. 6A; Christiansen and Ljungqvist, 2012; Moberg et al., 2005), and track sea surface temperature (Sicre et al., 2008) and drift ice in the North Atlantic (Fig. 6C; Bond et al., 2001). The linking mechanism is yet unclear, but may be related to solar activity. SST at sites 93KL and 275KL in the NE Arabian Sea gradually decreases over the mid to late Holocene, in accord with globally decreasing temperature (Marcott et al., 2013) and global SST cooling (PAGES/Ocean2k Working Group, 2012) and in response to decreasing NH summer insolation (Figs. 4C and 6D). Thus, NE monsoon strength closely mirrors long-term as well as centennial-scale variations in irradiance by responding to solar triggered feedback mechanisms such as the position of the ITCZ and Eurasian snow cover that determine the land-sea thermal contrast between the Asian continent and Indian Ocean.

In-step cooling over the North Atlantic, Asia and the Tibetan Plateau (Feng and Hu, 2005) triggered by reduced solar insolation leads to expanded snow cover over Eurasia, a delayed warming in spring and a reduced pressure gradient between central Asia and the southern Indian Ocean (Meehl, 1994). The reduced land-sea thermal contrast causes the SW monsoon to weaken, so that annual mean SST in the NE Arabian Sea is shifted to lower temperatures. A physical mechanism linking North Atlantic SST and monsoonal climate was recently proposed by Goswami et al. (2006): cold phases of the Atlantic Multidecadal Oscillation (AMO) result in a decrease of the meridional gradient of tropospheric temperature and thus to an early retreat of the SW monsoon, causing decreased monsoonal rainfall and low atmospheric temperatures in Asia (Wang et al., 2013). As pointed out above, this would enhance the influence of NE monsoonal winds and lower SST (sites 93KL

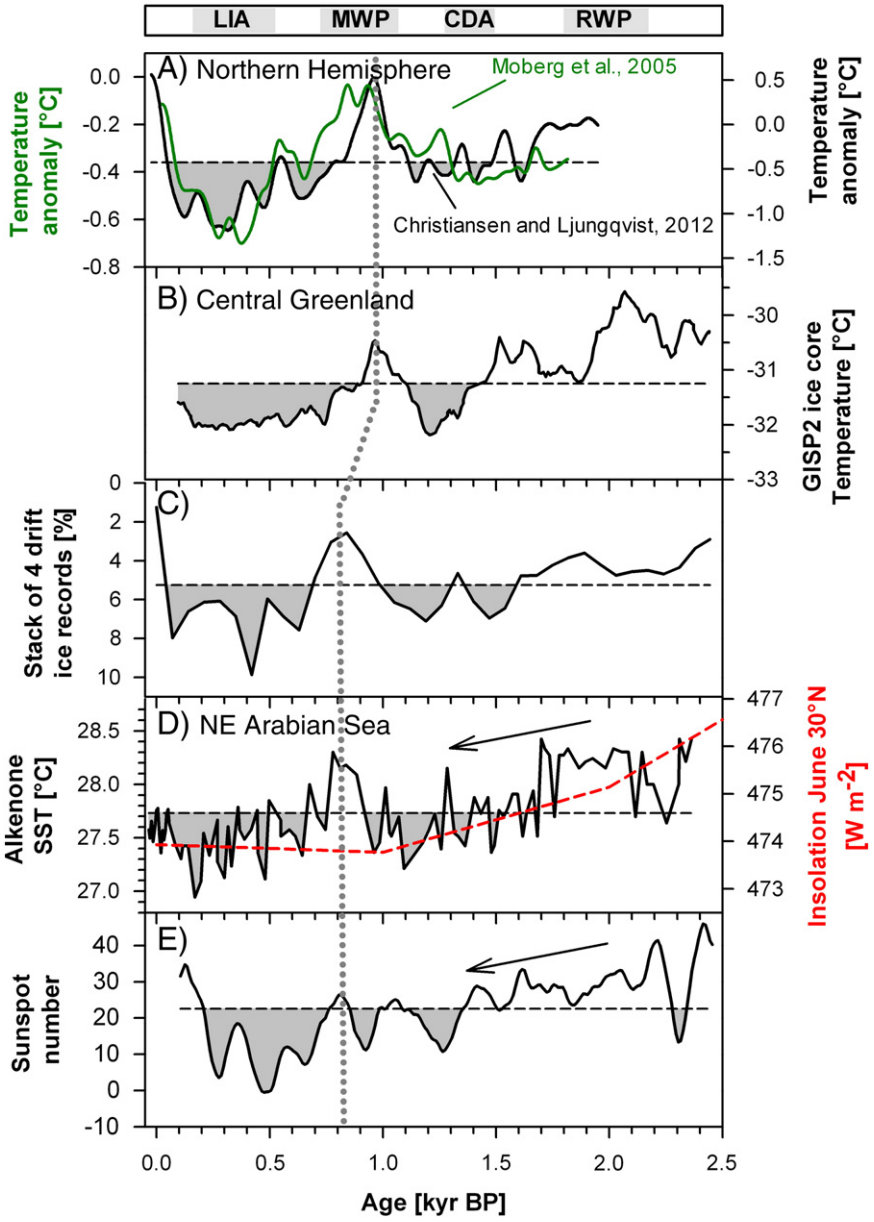

Fig. 6. A) Northern Hemisphere temperature reconstructions (Moberg et al., 2005; Christiansen and Ljungqvist, 2012), B) temperature record for Central Greenland from the GISP2 ice core (Alley, 2000), C) stack of 4 drift ice records from the North Atlantic (Bond et al., 2001), D) alkenone-SST record for cores 39KG/275KL from the northeastern Arabian Sea (black curve; Böll et al., 2014) compared to Northern Hemisphere summer solar insolation (red curve; Berger and Loutre, 1991), E) sunspot numbers (smoothed by a 11-point running mean) as an indicator for changes in solar output (Solanki et al., 2004). Dashed lines indicate the respective mean over the studied time interval.

and 275KL) off Pakistan. Although the exact teleconnection mechanism between climate variations of the high-latitude NH and the NE monsoon remains to be identified, SST in the northern Arabian Sea indicates that they are linked on orbital and shorter time scales during the Holocene.

5. Conclusions

Alkenone-based SST records from the NW Arabian Sea influenced by the summer monsoon (SST affected by upwelling processes) and from the NE Arabian Sea, where SST is mainly governed by the winter monsoon (no upwelling), depict the dynamic evolution of the SW and NE monsoon over the last 25 ka. The strength of summer monsoon activity was inversely related to winter monsoon intensity over the Holocene. SW monsoon intensity began to increase at the start of the last deglaciation and reached maximum strength between 11 and 8 ka during the early Holocene climate optimum, as indicated by SST changes offshore northern Oman. This is to our knowledge the first alkenone-based SST record that provides sufficient temporal resolution to show an early Holocene intensification of SW monsoon induced upwelling that caused lower than today annual mean SSTs in the northern Arabian Sea. The NE monsoon on the other hand was strongest during the Last Glacial Maximum but diminished since ~17 ka. Throughout the middle to late Holocene, SW monsoon activity weakened while the NE monsoon gained strength again. This interplay between SW and NE monsoon strength was forced by a southward displacement of the Intertropical Convergence Zone throughout the Holocene.

Millennial to centennial scale trends in monsoon strength over the northern Arabian Sea were linked to climate variations recorded on the Asian continent, such as variations in the East Asian monsoon and changes in air temperature. The increase of SST in the NE Arabian Sea during the last deglaciation lagged that of NH summer solar insolation and of Asian air temperature for about 3 ka because monsoon intensity was still influenced by glacial boundary conditions during this time. However, a strong linkage between northeast monsoonal wind strength over the northern Arabian Sea (as indicated by SST changes), temperature variations in Asia and climate of the high-latitude NH exists over the mid to late Holocene. Colder climate conditions over land increase the strength of northeast monsoonal winds and lower AM SST in the NE Arabian Sea. These centennial- to millennial-scale variations in the strength of the northeast monsoon over the northern Arabian Sea seem to be coupled to solar changes over the last 2000 years.

Acknowledgments

We are grateful to the German Federal Ministry of Education and Research (BMBF) for funding (BMBF grants 03G0806B, 03G0806C, 03G0806D, CARIMA). We wish to thank Catherine Kissel and the French coring team on board “Marion Dufresne” for taking the MD core. Reinhild Rosenberg is thanked for the routine high-quality preparation and measurement of alkenones. Two anonymous reviewers are thanked for very constructive comments that helped to improve this manuscript. Alkenone SST data of core SO130-275KL are available at www.pangaea.de (http://dx.doi.org/10.1594/PANGAEA.839067).

Appendix A. Supplementary data

Supplementary data to this article can be found online at http://dx.doi.org/10.1016/j.palaeo.2015.02.036.

References

Alley, R.B., 2000. The Younger Dryas cold interval as viewed from central Greenland. Quat. Sci. Rev. 19, 213–226.

Altabet, M.A., Higginson, M.J., Murray, D.W., 2002. The effect of millennial-scale changes in Arabian Sea denitrification on atmospheric CO_2. Nature 415, 159–162.

Anand, P., Kroon, D., Singh, A.D., Ganeshram, R.S., Ganssen, G., Elderfield, H., 2008. Coupled sea surface temperature–seawater $\delta^{18}O$ reconstructions in the Arabian Sea at the millennial scale for the last 35 ka. Paleoceanography 23, PA4207. http://dx.doi.org/10.1029/2007PA001564.

Anderson, D.M., Overpeck, J.T., Gupta, A.K., 2002. Increase in the Asian southwest monsoon during the past four centuries. Science 297, 596–599.

Anderson, D.M., Baulcomb, C.K., Duvivier, A.K., Gupta, A.K., 2010. Indian summer monsoon during the last two millennia. J. Quat. Sci. 25, 911–917. http://dx.doi.org/10.1002/jqs.1369.

Bao, Y., Bräuning, A., Yafeng, S., 2003. Late Holocene temperature fluctuations on the Tibetan Plateau. Quat. Sci. Rev. 22, 2335–2344. http://dx.doi.org/10.1016/S0277-3791(03)00132-X.

Berger, A., Loutre, M.F., 1991. Insolation values for the climate of the last 10 million years. Quat. Sci. Rev. 10, 297–317.

Böll, A., Lückge, A., Munz, P., Forke, S., Schulz, H., Ramaswamy, V., Rixen, T., Gaye, B., Emeis, K.-C., 2014. Late Holocene primary productivity and sea surface temperature variations in the northeastern Arabian Sea: implications for winter monsoon variability. Paleoceanography 29, 778–794. http://dx.doi.org/10.1002/2013PA002579.

Bond, G., Kromer, B., Beer, J., Muscheler, R., Evans, M.N., Showers, W., Hoffmann, S., Lotti-Bond, R., Hajdas, I., Bonani, G., 2001. Persistent solar influence on North Atlantic climate during the Holocene. Science 294, 2130–2136. http://dx.doi.org/10.1126/science.1065680.

Broccoli, A.J., Dahl, K.A., Stouffer, R.J., 2006. Response of the ITCZ to Northern Hemisphere cooling. Geophys. Res. Lett. 33, L01702. http://dx.doi.org/10.1029/2005GL024546.

Christiansen, B., Ljungqvist, F.C., 2012. The extra-tropical Northern Hemisphere temperature in the last two millennia: reconstructions of low-frequency variability. Clim. Past 8, 765–786. http://dx.doi.org/10.5194/cp-8-765-2012.

Clemens, S.C., Prell, W.L., 2003. A 350,000 year summer-monsoon multi-proxy stack from the Owen Ridge, Northern Arabian Sea. Mar. Geol. 201, 35–51. http://dx.doi.org/10.1016/S0025-3227(03)00207-X.

Clemens, S., Prell, W.L., Murray, D.W., Shimmield, G., Weedon, G., 1991. Forcing mechanisms of the Indian Ocean monsoon. Nature 353, 720–725.

Clemens, S.C., Prell, W.L., Sun, Y., 2010. Orbital-scale timing and mechanism driving Late Pleistocene Indo-Asian summer monsoons: reinterpreting cave speleothem $\delta^{18}O$. Paleoceanography 25. http://dx.doi.org/10.1029/2010PA001926.

Dahl, K.A., Oppo, D.W., 2006. Sea surface temperature pattern reconstructions in the Arabian Sea. Paleoceanography 21. http://dx.doi.org/10.1029/2005PA001162.

Dykoski, C., Edwards, R., Cheng, H., Yuan, D., Cai, Y., Zhang, M., Lin, Y., Qing, J., An, Z., Revenaugh, J., 2005. A high-resolution, absolute-dated Holocene and deglacial Asian monsoon record from Dongge Cave, China. Earth Planet. Sci. Lett. 233, 71–86. http://dx.doi.org/10.1016/j.epsl.2005.01.036.

Emeis, K.-C., Anderson, D.M., Doose-Rolinski, H., Kroon, D., Schulz-Bull, D., 1995. Sea-surface temperatures and the history of monsoon upwelling in the Northwest Arabian Sea during the last 500,000 years. Quat. Res. 43, 355–361.

Emeis, K.-C., Struck, U., Schulz, H.-M., Rosenberg, R., Bernasconi, S., Erlenkeuser, H., Sakamoto, T., Martinez-Ruiz, F., 2000. Temperature and salinity variations of Mediterranean Sea surface waters over the last 16,000 years from records of planktonic stable oxygen isotopes and alkenone unsaturation ratios. Palaeogeogr. Palaeoclimatol. Palaeoecol. 158, 259–280.

Esper, J., Schweingruber, F.H., Winiger, M., 2002. 1300 years of climate history for Western Central Asia inferred from tree-rings. The Holocene 12, 267–277.

Fang, X.-M., Ono, Y., Fukusawa, H., Bao-Tian, P., Li, J.-J., Dong-Hong, G., Oi, K., Tsukamoto, S., Torii, M., Mishima, T., 1999. Asian summer monsoon instability during the past 60,000 years: magnetic susceptibility and pedogenic evidence from the western Chinese Loess Plateau. Earth Planet. Sci. Lett. 168, 219–232.

Feng, S., Hu, Q., 2005. Regulation of Tibetan Plateau heating on variation of Indian summer monsoon in the last two millennia. Geophys. Res. Lett. 32, L02702. http://dx.doi.org/10.1029/2004GL021246.

Fleitmann, D., Burns, S.J., Mudelsee, M., Neff, U., Kramers, J., Mangini, A., Matter, A., 2003. Holocene forcing of Indian monsoon recorded in a stalagmite from Southern Oman. Science 300, 1737–1739.

Fleitmann, D., Burns, S.J., Neff, U., Mudelsee, M., Mangini, A., Matter, A., 2004. Palaeoclimatic interpretation of high-resolution oxygen isotope profiles derived from annually laminated speleothems from Southern Oman. Quat. Sci. Rev. 23, 935–945.

Fleitmann, D., Burns, S.J., Mangini, A., Mudelsee, M., Kramers, J., Villa, I., Neff, U., Al-Subbary, A.A., Buettner, A., Hippler, D., Matter, A., 2007. Holocene ITCZ and Indian monsoon dynamics recorded in stalagmites from Oman and Yemen (Socotra). Quat. Sci. Rev. 26, 170–188. http://dx.doi.org/10.1016/j.quascirev.2006.04.012.

Fuchs, M., Buerkert, A., 2008. A 20 ka sediment record from the Hajar Mountain range in N-Oman, and its implication for detecting arid–humid periods on the southeastern Arabian Peninsula. Earth Planet. Sci. Lett. 265, 546–558. http://dx.doi.org/10.1016/j.epsl.2007.10.050.

Ge, Q., Hao, Z., Zheng, J., Shao, X., 2013. Temperature changes over the past 2000 yr in China and comparison with the Northern Hemisphere. Clim. Past 9, 1153–1160. http://dx.doi.org/10.5194/cp-9-1153-2013.

Goswami, B.N., Madhusoodanan, M.S., Neema, C.P., Sengupta, D., 2006. A physical mechanism for North Atlantic SST influence on the Indian summer monsoon. Geophys. Res. Lett. 33, L02706. http://dx.doi.org/10.1029/2005GL024803.

Grootes, P.M., Stuiver, M., 1997. Oxygen 18/16 variability in Greenland snow and ice with 10^{-3}- to 10^{5}-year time resolution. J. Geophys. Res. 102, 26455–26470.

Gupta, A.K., Anderson, D.M., Overpeck, J.T., 2003. Abrupt changes in the Asian southwest monsoon during the Holocene and their links to the North Atlantic Ocean. Nature 421, 354–356.

Gupta, A.K., Das, M., Anderson, D.M., 2005. Solar influence on the Indian summer monsoon during the Holocene. Geophys. Res. Lett. 32. http://dx.doi.org/10.1029/2005GL022685.

Gupta, A.K., Mohan, K., Sarkar, S., Clemens, S.C., Ravindra, R., Uttam, R.K., 2011. East–West similarities and differences in the surface and deep northern Arabian Sea records

during the past 21 kyr. Palaeogeogr. Palaeoclimatol. Palaeoecol. 301, 75–85. http://dx.doi.org/10.1016/j.palaeo.2010.12.027.
Haake, B., Ittekkot, V., Rixen, T., Ramaswamy, V., Nair, R.R., Curry, W.B., 1993. Seasonality and interannual variability of particle fluxes to the deep Arabian Sea. Deep-Sea Res. I 40, 1323–1344.
Hastenrath, S., Lamb, P.J., 1979. Climate atlas of the Indian Ocean. Surface Climate and Atmospheric Circulation. vol.1. University of Wisconsin Press, Madison.
Haug, G.H., Hughen, K.A., Sigman, D.M., Peterson, L.C., Röhl, U., 2001. Southward migration of the intertropical convergence zone through the Holocene. Science 293, 1304–1308. http://dx.doi.org/10.1126/science.1059725.
Herzschuh, U., 2006. Palaeo-moisture evolution in monsoonal Central Asia during the last 50,000 years. Quat. Sci. Rev. 25, 163–178. http://dx.doi.org/10.1016/j.quascirev.2005.02.006.
Hong, Y.T., Hong, B., Lin, Q.H., Zhu, Y.X., Shibata, Y., Hirota, M., Uchida, M., Leng, X.T., Jiang, H.B., Xu, H., Wang, H., Yi, L., 2003. Correlation between Indian Ocean summer monsoon and North Atlantic climate during the Holocene. Earth Planet. Sci. Lett. 211, 371–380.
Huguet, C., Kim, J.-H., Sinninghe Damsté, J.S., Schouten, S., 2006. Reconstruction of sea surface temperature variations in the Arabian Sea over the last 23 kyr using organic proxies (TEX_{86} and $U^{K'}_{37}$). Paleoceanography 21, PA3003. http://dx.doi.org/10.1029/2005PA001215.
Ivanochko, T., Ganeshram, R.S., Brummer, G.-J.A., Ganssen, G., Jung, S.J.A., Moreton, S.G., Kroon, D., 2005. Variations in tropical convection as an amplifier of global climate change at the millennial scale. Earth Planet. Sci. Lett. 235, 302–314. http://dx.doi.org/10.1016/j.epsl.2005.04.002.
Kessarkar, P.M., Purnachadra Rao, V., Naqvi, S.W.A., Karapurkar, S.G., 2013. Variation in the Indian summer monsoon intensity during the Bølling–Ållerød and Holocene. Paleoceanography 28. http://dx.doi.org/10.1002/palo.20040.
Lambeck, K., 1996. Shoreline reconstructions for the Persian Gulf since the last glacial maximum. Earth Planet. Sci. Lett. 142, 43–57. http://dx.doi.org/10.1016/0012-821X(96)00069-6.
Levitus, S., Boyer, T., 1994. World Ocean Atlas 1994, vol. 4. Temperature, NOAA Atlas NESDIS. vol.4. U.S. department of Commerce, Washington, D.C.
Lézine, A.-M., Tiercelin, J.-J., Robert, C., Saliège, J.-F., Cleuziou, S., Inizan, M.-L., Braemer, F., 2007. Centennial to millennial-scale variability of the Indian monsoon during the early Holocene from a sediment, pollen and isotope record from the desert of Yemen. Palaeogeogr. Palaeoclimatol. Palaeoecol. 243, 235–249. http://dx.doi.org/10.1016/j.palaeo.2006.05.019.
Liu, X., Dong, H., Yang, X., Herzschuh, U., Zhang, E., Stuut, J.-B.W., Wang, Y., 2009. Late Holocene forcing of the Asian winter and summer monsoon as evidenced by proxy records from the northern Qinghai–Tibetan Plateau. Earth Planet. Sci. Lett. 280, 276–284. http://dx.doi.org/10.1016/j.epsl.2009.01.041.
Lückge, A., Doose-Rolinski, H., Khan, A.A., Schulz, H., von Rad, U., 2001. Monsoonal variability in the northeastern Arabian Sea during the past 5000 years: geochemical evidence from laminated sediments. Palaeogeogr. Palaeoclimatol. Palaeoecol. 167, 273–286.
Madhupratap, M., Prasanna Kumar, S., Bhattathiri, P.M.A., Dileep Kumar, M., Raghukumar, S., Nair, K.K.C., Ramaiah, N., 1996. Mechanism of the biological response to winter cooling in the northeastern Arabian Sea. Nature 384, 549–552.
Marathayil, D., Turner, A.G., Shaffrey, L.C., Levine, R.C., 2013. Systematic winter sea-surface temperature biases in the northern Arabian Sea in HiGEM and the CMIP3 models. Environ. Res. Lett. 8, 014028. http://dx.doi.org/10.1088/1748-9326/8/1/014028.
Marcott, S.A., Shakun, J.D., Clark, P.U., Mix, A.C., 2013. A reconstruction of regional and global temperature for the past 11,300 years. Science 339, 1198–1201. http://dx.doi.org/10.1126/science.1228026.
Meehl, G.A., 1994. Influence of the land surface in the Asian summer monsoon: external conditions versus internal feedbacks. J. Clim. 7, 1033–1049.
Moberg, A., Sonechkin, D.M., Holmgren, K., Datsenko, N.M., Karlén, W., 2005. Highly variable Northern Hemisphere temperatures reconstructed from low- and high-resolution proxy data. Nature 433, 613–617. http://dx.doi.org/10.1038/nature03298.1.
Naidu, P.D., Malmgren, A., 1996. A high-resolution record of late Quaternary upwelling along the Oman Margin, Arabian Sea based on planktonic foraminifera. Palaeogeography 11, 129–140. http://dx.doi.org/10.1029/95PA03198.
Naidu, P.D., Malmgren, B.A., 2005. Seasonal sea surface temperature contrast between the Holocene and last glacial period in the western Arabian Sea (Ocean Drilling Project Site 723A): modulated by monsoon upwelling. Paleoceanography 20. http://dx.doi.org/10.1029/2004PA001078.
Neff, U., Burns, S.J., Mangini, A., Mudelsee, M., Fleitmann, D., Matter, A., 2001. Strong coherence between solar variability and the monsoon in Oman between 9 and 6 kyr ago. Nature 411, 290–293. http://dx.doi.org/10.1038/35077048.
Overpeck, J., Anderson, D., Trumbore, S., Prell, W., 1996. The southwest Indian monsoon over the last 18,000 years. Clim. Dyn. 12, 213–225. http://dx.doi.org/10.1007/BF00211619.
PAGES 2k Consortium, 2013. Continental-scale temperature variability during the past two millennia. Nat. Geosci. 6, 339–346. http://dx.doi.org/10.1038/NGEO1797.
PAGES/Ocean2k Working Group, 2012. Synthesis of marine sediment-derived SST records for the past 2 millennia: first-order results from the PAGES/Ocean2k project. AGU Fall Meet. abstr. (PP1)
Peterse, F., Prins, M.A., Beets, C.J., Troelstra, S.R., Zheng, H., Gu, Z., Schouten, S., Sinninghe Damste, J.S., 2011. Decoupled warming and monsoon precipitation in East Asia over the last deglaciation. Earth Planet. Sci. Lett. 301, 256–264. http://dx.doi.org/10.1016/j.epsl.2010.11.010.
Pichevin, L., Bard, E., Martinez, P., Billy, I., 2007. Evidence of ventilation changes in the Arabian Sea during the late Quaternary: implication for denitrification and nitrous oxide emission. Glob. Biogeochem. Cycles 21. http://dx.doi.org/10.1029/2006GB002852.
Pourmand, A., Marcantonio, F., Schulz, H., 2004. Variations in productivity and eolian fluxes in the northeastern Arabian Sea during the past 110 ka. Earth Planet. Sci. Lett. 221, 39–54. http://dx.doi.org/10.1016/S0012-821X(04)00109-8.
Pourmand, A., Marcantonio, F., Bianchi, T.S., Canuel, E.A., Waterson, E.J., 2007. A 28-ka history of sea surface temperature, primary productivity and planktonic community variability in the western Arabian Sea. Paleoceanography 22, PA4208. http://dx.doi.org/10.1029/2007PA001502.
Prasanna Kumar, S., Prasad, T.G., 1996. Winter cooling in the northern Arabian Sea. Curr. Sci. 71, 834–841.
Reichart, G.J., Lourens, L.J., Zachariasse, W.J., 1998. Temporal variability in the northern Arabian Sea Oxygen Minimum Zone (OMZ) during the last 225,000 years. Paleoceanography 13, 607–621.
Reichart, G.J., Schenau, S.J., de Lange, G.J., Zachariasse, W.J., 2002. Synchroneity of oxygen minimum zone intensity on the Oman and Pakistan Margins at sub-Milankovitch time scales. Mar. Geol. 185, 403–415. http://dx.doi.org/10.1016/S0025-3227(02)00184-6.
Rixen, T., Haake, B., Ittekkot, V., Guptha, M.V.S., Nair, R.R., Schlüssel, P., 1996. Coupling between SW monsoon-related surface and deep ocean processes as discerned from continuous particle flux measurements and correlated satellite data. J. Geophys. Res. 101, 569–582.
Rixen, T., Ittekkot, V., Haake-Gaye, B., Schäfer, P., 2000. The influence of the SW monsoon on the deep-sea organic carbon cycle in the Holocene. Deep-Sea Res. II 47, 2629–2651.
Rixen, T., Baum, A., Gaye, B., Nagel, B., 2014. Seasonal and interannual variations in the nitrogen cycle in the Arabian Sea. Biogeosciences 11, 5733–5747. http://dx.doi.org/10.5194/bg-11-5733-2014.
Rostek, F., Bard, E., Beaufort, L., Sonzogni, C., Ganssen, G., 1997. Sea surface temperature and productivity records for the past 240 kyr in the Arabian Sea. Deep-Sea Res. II 44, 1461–1480.
Saher, M.H., Jung, S.J.A., Elderfield, H., Greaves, M.J., Kroon, D., 2007a. Sea surface temperatures of the western Arabian Sea during the last deglaciation. Paleoceanography 22, PA2208. http://dx.doi.org/10.1029/2006PA001292.
Saher, M.H., Peeters, F.J.C., Kroon, D., 2007b. Sea surface temperatures during the SW and NE monsoon seasons in the western Arabian Sea over the past 20,000 years. Palaeogeogr. Palaeoclimatol. Palaeoecol. 249, 216–228. http://dx.doi.org/10.1016/j.palaeo.2007.01.014.
Saraswat, R., Lea, D.W., Nigam, R., Mackensen, A., Naik, D.K., 2013. Deglaciation in the tropical Indian Ocean driven by interplay between the regional monsoon and global teleconnections. Earth Planet. Sci. Lett. 375, 166–175. http://dx.doi.org/10.1016/j.epsl.2013.05.022.
Schlitzer, R., 2013. Ocean Data View. http://odv.awi-bremerhaven.de.
Schulte, S., Müller, P., 2001. Variations of sea surface temperature and primary productivity during Heinrich and Dansgaard–Oeschger events in the northeastern Arabian Sea. Geo-Mar. Lett. 21, 168–175. http://dx.doi.org/10.1007/s003670100080.
Schulz, H., von Rad, U., Erlenkeuser, H., 1998. Correlation between Arabian Sea and Greenland climate oscillations of the past 110,000 years. Nature 393, 54–57.
Schulz, H., Emeis, K.-C., Erlenkeuser, H., von Rad, U., Rolf, C., 2002. The Toba volcanic event and interstadial/stadial climates at the marine isotopic stage 5 to 4 transition in the Northern Indian Ocean. Quat. Res. 57, 22–31.
Sicre, M.-A., Jacob, J., Ezat, U., Rousse, S., Kissel, C., Yiou, P., Eiríksson, J., Knudsen, K.L., Jansen, E., Turon, J.-L., 2008. Decadal variability of sea surface temperatures off North Iceland over the last 2000 years. Earth Planet. Sci. Lett. 268, 137–142. http://dx.doi.org/10.1016/j.epsl.2008.01.011.
Sirocko, F., Sarnthein, M., Erlenkeuser, H., Lange, H., Arnold, M., Duplessy, J.C., 1993. Century-scale events in monsoonal climate over the past 24,000 years. Nature 364, 322–324.
Solanki, S.K., Usoskin, I.G., Kromer, B., Schüssler, M., Beer, J., 2004. Unusual activity of the sun during recent decades compared to the previous 11,000 years. Nature 431, 1084–1087. http://dx.doi.org/10.1038/nature02995.
Sonzogni, C., Bard, E., Rostek, F., Lafont, R., Rosell-Mele, A., Eglinton, G., 1997. Core-top calibrations of the alkenone index vs sea surface temperature in the Indian Ocean. Deep-Sea Res. II 44, 1445–1460.
Sonzogni, C., Bard, E., Rostek, F., 1998. Tropical sea-surface temperatures during the last glacial period: a view based on alkenones in Indian Ocean sediments. Quat. Sci. Rev. 17, 1185–1201.
Suthhof, A., Ittekkot, V., Gaye-Haake, B., 2001. Millennial-scale oscillation of denitrification intensity in the Arabian Sea during the late Quaternary and its potential influence on atmospheric N_2O and global climate. Global Biogeochem. Cycles 1–13.
Thompson, L.G., Yao, T., Davis, M.E., Henderson, K.A., Mosley-Thompson, E., Lin, P.-N., Beer, J., Synal, H.-A., Cole-Dai, J., Bolzan, J.F., 1997. Tropical climate instability: the last glacial cycle from a Qinghai–Tibetan ice core. Science 276, 1821–1825. http://dx.doi.org/10.1126/science.276.5320.1821.
Van Rampelbergh, M., Fleitmann, D., Verheyden, S., Cheng, H., Edwards, L., De Geest, P., De Vleeschouwer, D., Burns, S.J., Matter, A., Claeys, P., Keppens, E., 2013. Mid- to late Holocene Indian Ocean Monsoon variability recorded in four speleothems from Socotra Island, Yemen. Quat. Sci. Rev. 65, 129–142. http://dx.doi.org/10.1016/j.quascirev.2013.01.016.
von Rad, U., Burgarth, K.-P., Pervaz, M., Schulz, H., 2002. Discovery of the Toba ash (c. 70 ka) in a high-resolution core recovering millennial monsoonal variability off Pakistan. Geol. Soc. London Spec. Publ. 195, 445–461.
Wang, Y.J., Cheng, H., Edwards, R.L., An, Z.S., Wu, J.Y., Shen, C.C., Dorale, J.A., 2001. A high-resolution absolute-dated late Pleistocene Monsoon record from Hulu Cave, China. Science 294, 2345–2348. http://dx.doi.org/10.1126/science.1064618.
Wang, P., Clemens, S.C., Beaufort, L., Braconnot, P., Ganssen, G., Zhimin, J., Kershaw, P., Sarnthein, M., 2005a. Evolution and variability of the Asian monsoon system: state of the art and outstanding issues. Quat. Sci. Rev. 24, 595–629.

Wang, Y., Cheng, H., Edwards, R.L., He, Y., Kong, X., An, Z., Wu, J., Kelly, M.J., Dykoski, C.A., Li, X., 2005b. The Holocene Asian monsoon: links to solar changes and North Atlantic climate. Science 308, 854–857. http://dx.doi.org/10.1126/science.1106296.

Wang, J., Yang, B., Ljungqvist, F.C., Zhao, Y., 2013. The relationship between the Atlantic Multidecadal Oscillation and temperature variability in China during the last millennium. J. Quat. Sci. http://dx.doi.org/10.1002/jqs.2658.

Wen, R., Xiao, J., Chang, Z., Zhai, D., Xu, Q., Li, Y., Itoh, S., 2010. Holocene precipitation and temperature variations in the East Asian monsoonal margin from pollen data from Hulun Lake in northeastern Inner Mongolia, China. Boreas 39, 262–272. http://dx.doi.org/10.1111/j.1502-3885.2009.00125.x.

Yancheva, G., Nowaczyk, N.R., Mingram, J., Dulski, P., Schettler, G., Negendank, J.F.W., Liu, J., Sigman, D.M., Peterson, L.C., Haug, G.H., 2007. Influence of the intertropical convergence zone on the East Asian monsoon. Nature 445, 74–77. http://dx.doi.org/10.1038/nature05431.

Yang, B., Bräuning, A., Johnson, K.R., Yafeng, S., 2002. General characteristics of temperature variation in China during the last two millennia. Geophys. Res. Lett. 29. http://dx.doi.org/10.1029/2001GL014485.